Isoscaling behavior in fission dynamics

Y. G. Ma,[1,*] K. Wang,[1,2] X. Z. Cai,[1] J. G. Chen,[1,2] J. H. Chen,[1,2] D. Q. Fang,[1] W. Guo,[1,2] C. W. Ma,[1,2] G. L. Ma,[1,2] W. Q. Shen,[1] Q. M. Su,[1,2] W. D. Tian,[1] Y. B. Wei,[1,2] T. Z. Yan,[1,2] C. Zhong,[1] X. F. Zhou,[1,3] and J. X. Zuo[1,2]

[1]*Shanghai Institute of Applied Physics, Chinese Academy of Sciences, P.O. Box 800-204, Shanghai 201800, China*

[2]*Graduate School of the Chinese Academy of Sciences, China*

[3]*College of Sciences, Ningbo University, Zhejiang 315211, China*

(Received 13 December 2004; revised manuscript received 5 October 2005; published 8 December 2005)

The fission processes of ^{112}Sn+^{112}Sn and ^{116}Sn+^{116}Sn are simulated with the combination of the Langevin equation and the statistical decay model. The masses of two fission fragments are given by assuming the process of symmetric fission or asymmetric fission by Monte Carlo sampling with the Gaussian probability distribution. From the analysis of the isotopic/isotonic ratios of the fission fragments from both reactions, the isoscaling behavior has been observed and investigated in detail. Isoscaling parameters α and β are extracted as a function of the charge number and neutron number, respectively, in different widths of the sampling Gaussian probability distribution. It seems that α is sensitive to the width of fission probability distribution of the mass asymmetrical parameter, but β is not. Both α and β drop with increasing beam energy and reduced friction parameter.

DOI: 10.1103/PhysRevC.72.064603 PACS number(s): 24.75.+i, 25.85.Ge, 21.10.Tg

I. INTRODUCTION

The availability of exotic nuclear beams with extreme neutron-to-proton ratios provides an opportunity to explore the collision dynamics of isospin-asymmetric nuclear systems [1]. To facilitate this kind of study, the suitable selection of the sensitive experimental observables related to the isospin degree of freedom is one of the key points. One such observable is the isotopic/isobaric ratio [2,3], which has been used before to probe the isospin equilibration at medium energies. Recently, this kind of ratio has been systematically revisited for two different reactions with the same charge number and similar temperature, and a so-called isoscaling law has been observed experimentally [4–6]. Isoscaling means that the ratio of isotope yields from two different reactions, 1 and 2, $R_{21}(N, Z) = Y_2(N, Z)/Y_1(N, Z)$, is found to exhibit an exponential relationship as a function of the neutron number N and proton number Z [4]

$$R_{21}(N, Z) = \frac{Y_2(N, Z)}{Y_1(N, Z)} = C \exp(\alpha N + \beta Z), \qquad (1)$$

where C, α, and β are parameters. In the grand-canonical limit, $\alpha = \Delta\mu_n/T$ and $\beta = \Delta\mu_z/T$, where $\Delta\mu_n$ and $\Delta\mu_z$ are the differences between the neutron and proton chemical potentials for two reactions, respectively. This behavior is attributed to the difference of two reaction systems with different isospin asymmetry. It is possible to probe the isospin-dependent nuclear equation of state by the studies of isoscaling [7]. So far, the isoscaling behavior has been experimentally explored in various reaction mechanisms, ranging from the evaporation [4], fission [8,9], and deep inelastic reactions at low energies to the projectile fragmentation [10,11] and multifragmentation at intermediate energy [4,12,13]. Also, the isoscaling phenomenon has been extensively examined in different theoretical frameworks ranging from dynamical transport models, such as the Blotzmann-Uehling-Uhlenbeck model [12], quantum molecular dynamics model [14], and antisymmetrical molecular dynamics model [15], to the statistical models, such as the expansion emission source model, the statistical multifragmentation model, and the lattice gas model [5,6,16–18]. In this work, we will focus on the detailed simulation studies of the isoscaling behavior of the fission fragments. A brief report has been published recently [19].

In this work, we present an analysis of fragments from the fission process as simulated by the Langevin equation. The isotopic or isotonic ratios of the different fragment yields from the ^{116}Sn+^{116}Sn and ^{112}Sn+^{112}Sn systems are presented, and the features of isoscaling behavior in fission dynamics are investigated.

The paper is organized by the following structure. In Sec. II, a brief description of the Langevin model is given and the partition of masses of two fission fragments is assumed. In Sec. III, the detailed results for the fission-fragment isotopic and isotonic distribution are presented and the isoscaling behavior is explored. Finally, we summarize this work in Sec. IV.

II. BRIEF DESCRIPTION OF THE LANGEVIN MODEL

The process of fission can be described in terms of collective motion using the transport theory [20–24]. The dynamics of the collective degrees of freedom is typically described using the Langevin or Fokker-Planck equation. In this work, we deal with a combined dynamical and statistical model (CDSM) which is a combination of a dynamical Langevin equation and a statistical model to describe the fission process of a heavy ion reaction [21]. This model is an overdamped Langevin equation coupled with a Monte Carlo procedure allowing for the discrete emission of light particles. It switches over to a statistical model when the dynamical description reaches a quasistationary regime.

We first specify the entrance channel through which a compound nucleus is formed, i.e., the target and projectile is complete fusion. The fusion process for simulating fission

*E-mail: ygma@sinap.ac.cn

in each trajectory with angular momentum $L = \hbar l$ is described by

$$\sigma(l) = \frac{2\pi}{k^2} \frac{2l+1}{1+\exp[(l-l_c)/\delta_l]}, \tag{2}$$

where the parameters l_c and δl are according to an approximating scaling of Ref. [20]. Namely,

$$l_c = \sqrt{A_P A_T / A_{\rm CN}}\left(A_P^{1/3} + A_T^{1/3}\right)\left(0.33 + 0.205\sqrt{E_{\rm c.m.} - V_c}\right), \tag{3}$$

when $0 < E_{\rm c.m.} - V_c < 120$ MeV; and when $E_{\rm c.m.} - V_c > 120$ MeV, the term in the last bracket is set equal to 2.5. In Eq. (3), A_T and A_P represent the mass of the target and projectile, respectively; and $A_{\rm CN}$ is the mass of the compound nucleus. For the barrier V_c, the following ansatz is used:

$$V_c = \frac{5}{3} c_3 \frac{Z_P Z_T}{A_P^{1/3} + A_T^{1/3} + 1.6}, \tag{4}$$

with $c_3 = 0.7053$ MeV. The diffuseness δl is found to scale as

$$\delta l = \begin{cases} \left[(A_P A_T)^{3/2} \times 10^{-5}\right][1.5 + 0.02(E_{\rm c.m.} - V_c - 10)] & \text{for} \quad E_{\rm c.m.} > V_c + 10, \\ \left[(A_P A_T)^{3/2} \times 10^{-5}\right][1.5 - 0.04(E_{\rm c.m.} - V_c - 10)] & \text{for} \quad E_{\rm c.m.} < V_c + 10. \end{cases}$$

A trajectory with the particular angular momentum L is started at the ground-state position $q_{\rm gs}$ of the entropy $S(q_{\rm gs}, E^*_{\rm tot}, A, Z, L)$, q is half of the distance between the centers of masses of the future fission fragments. In this work, the total initial excitation energy $E^*_{\rm tot}$ is given by $E^*_{\rm tot} = E_{\rm beam} A_T/(A_T + A_P) + Q$, where Q is the fusion Q value calculated by $Q = M_T + M_P - M^{\rm LD}_{\rm CN}$. M_T and M_P are the masses of the projectile and target, which come from experimental data. If the mass is unavailable, it is calculated by a macroscopic-microscopic model [25]. $M^{\rm LD}_{\rm CN}$ is the mass of the compound nucleus, which is calculated from the liquid-drop model.

The dynamical part of the CDSM model is described by the Langevin equation which is driven by the free energy F. In the Fermi gas model, F is related to the level density parameter $a(q)$ [26] by

$$F(q, T) = V(q) - a(q)T^2, \tag{5}$$

where $V(q)$ is the fission potential and T is the nuclear temperature.

The overdamped Langevin equation reads

$$\frac{dq}{dt} = -\frac{1}{M\beta_0(q)}\left(\frac{\partial F(q,T)_T}{\partial q}\right) + \sqrt{D(q)}\Gamma(t), \tag{6}$$

where q is the dimensionless fission coordinate defined above. $\beta_0(q)$ is the reduced friction parameter, which is the only parameter of this model. The fluctuation strength coefficient $D(q)$ can be expressed according to the fluctuation-dissipation theorem as

$$D(q) = \frac{T}{M\beta_0(q)}, \tag{7}$$

where M is the inertia parameter which drops out of the overdamped equation. $\Gamma(t)$ is a time-dependent stochastic variable with Gaussian distribution. Its average and correlation function are written as

$$\begin{aligned} \langle\Gamma(t)\rangle &= 0, \\ \langle\Gamma(t)\Gamma(t')\rangle &= 2\delta_\varepsilon(t - t'). \end{aligned} \tag{8}$$

The potential energy $V(A, Z, L, q)$ is obtained from the finite-range liquid-drop model [27]

$$\begin{aligned} V(A,Z,L,q) = a_2\left[1 - k\left(\frac{N-Z}{A}\right)^2\right]A^{2/3}[B_s(q) - 1] \\ + c_3\frac{Z^2}{A^{1/3}}[B_c(q) - 1] + c_r L^2 A^{-5/3} B_r(q), \end{aligned} \tag{9}$$

where $B_s(q)$, $B_c(q)$, and $B_r(q)$ are surface, Coulomb, and rotational energy terms, respectively, which depend on the deformation coordinate q. a_2, c_3, k, and c_r are parameters not related to q. In our calculation, we take them according to Ref. [20] to be.

$$\begin{aligned} a_2 &= 17.9439\,\text{MeV}, \quad & c_3 &= 0.7053\,\text{MeV}, \\ k &= 1.7826, & c_r &= 34.50\,\text{MeV}. \end{aligned}$$

We use c and h [28] to describe the shape of the nucleus in

$$\rho^2(z) = \left(1 - \frac{z^2}{c_0^2}\right)\left[\left(\frac{1}{c^3} - \frac{b_0}{5}\right)c_0^2 + B_{\rm sh}(c,h)z^2\right], \tag{10}$$

where

$$c_0 = cR, \qquad R = 1.16A^{1/3}. \tag{11}$$

The nuclear shape function $B_{\rm sh}(c, h)$ and the collective fission coordinate $q(c, h)$ of mass number A are expressed as

$$\begin{aligned} B_{\rm sh}(c,h) &= 2h + \frac{c-1}{2}, \\ q(c,h) &= \frac{3}{8}c\left[1 + \frac{2}{15}B_{\rm sh}(c,h)c^3\right]. \end{aligned} \tag{12}$$

The fission process of the Langevin equation is propagated using an interpretation of Smoluchowski [29] ($\lambda = 1$ in the following equation) which is consistent with the kinetic form which reads

$$\begin{aligned} q_{n+1} = q_n + \left[\frac{T(q)}{\beta_0(q)M}\frac{dS(q)}{dq}\right]_n \tau + \lambda\left[\frac{d}{dq}\left(\frac{T(q)}{\beta_0(q)M}\right)\right]_n \tau \\ + \sqrt{\left[\frac{T(q)}{\beta_0(q)M}\right]_n \tau}\, w_n. \end{aligned} \tag{13}$$

Here τ is the time step of the Langevin equation, w_n is a Gaussian-distributed random number with variance 2. $S(q) = 2\sqrt{a(q, A)[E_{\rm tot} - V(q, A, Z, l)]}$ is the entropy. The parameter λ allows us to distinguish between the different possibilities to discretize the Langevin equation. It is called *interpretation* in the literature. In the analysis of the experiments on fission of hot nuclei discussed in the reviews [20,30] and in the papers quoted there, the Itô-interpretation ($\lambda = 0$) [31] has been used exclusively. Also there are other interpretations, namely, that of Stratonovich [32] ($\lambda = 1/2$), or an interpretation consistent with the kinetic form of the Smoluchowski equation of [29] ($\lambda = 1$). In this work, we take $\lambda = 1$.

In our calculation, we adopt the one-body dissipation (OBD) friction form factor $\beta_{\rm OBD}$ [33] as $\beta_0(q)$ which is calculated with one-body dissipation with a reduction of the wall term except for the special case which we claim. Here we use an analytical fit formula developed in Ref. [34], i.e.,

$$\beta_{\rm OBD}(q) = \begin{cases} 15/q^{0.43} + 1 - 10.5q^{0.9} + q^2 & \text{if} \quad q > 0.38, \\ 32 - 32.21q & \text{if} \quad q < 0.38. \end{cases}$$

In the dynamical part of the model, the emission of light particles (n, p, d, α) and giant dipole γ are calculated at each Langevin time step τ; the widths for particle and giant dipole γ decay are given by the parametrization of Blann [35] and Lynn [36], respectively.

III. RESULTS AND DISCUSSIONS

A. Isotopic/isotonic distributions of the fission fragments

In Figs. 1(a) and 1(b), we demonstrate the ratio of the prescission neutron number R_N and of the pre-scission proton number R_P between ^{116}Sn+^{116}Sn and ^{112}Sn+^{112}Sn, respectively, as a function of beam energy ($E_{\rm beam}/A$). First, the values of R_N are larger than 1 while those of R_P are less than 1, indicating that the neutron is easier to be emitted for the neutron-rich system while the proton is in a contrary trend. Of course, this is a natural result of the chemical composition of the reaction system [37,38]. Second, with the increasing beam energy, R_N shows a decreasing trend while R_P increases, which can be interpreted to mean that the isospin effect weakens as the beam energy rises up.

Within the framework of the Langevin simulation, we chose 200 000 fission events which happen on the dynamic channel (we gave up the events that happen in the statistical part of CDSM model) and chose a Gaussian-distributed random number as the mass asymmetry parameter $\alpha_0 = \frac{A_1 - A_2}{A_1 + A_2}$ when the system reaches the scission point. When $\alpha_0 = 0$, it means the fission is symmetrical. It is taken from a Gaussian-distributed random number from -1 to 1 with the mean value of zero. A_1 and A_2 are the masses of the two fission fragments. In this work, we assume the fission fragments have the same N/Z as that of the initial system, and then Z_1 or Z_2 of the fission fragments can be deduced from A_1 or A_2. This assumption is similar to the case of deep inelastic heavy ion collisions at low energies, where the isospin degree of freedom has been found to reach equilibrium first [39]. Figure 2 shows the mass distribution of the fission fragments from ^{112}Sn+^{112}Sn and ^{116}Sn+^{116}Sn reaction systems assuming the different width of the sampling Gaussian probability for the mass asymmetrical parameter of fission fragments σ_{α_0}. Naturally, the bigger the σ_{α_0}, the wider the fragment mass distributions.

Samples for the isotopic and isotonic distributions in some given Z and N are shown in Fig. 3. The square of the full widths of these distributions shows a systematic increase with Z or N as shown in Fig. 4, and the absolute value of the differences of the centroid of the isotonic/isotopic distributions shows an increasing trend, too (see later in Fig. 6). Apparently, the widths are not sensitive to the width of the Gaussian probability for

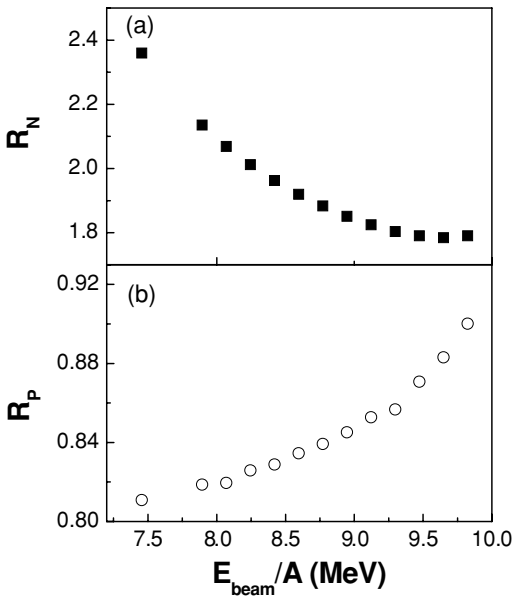

FIG. 1. Ratios of the pre-scission neutron number (a) and of the pre-scission proton number (b) between ^{116}Sn+^{116}Sn and ^{112}Sn+^{112}Sn as a function of beam energy ($E_{\rm beam}/A$).

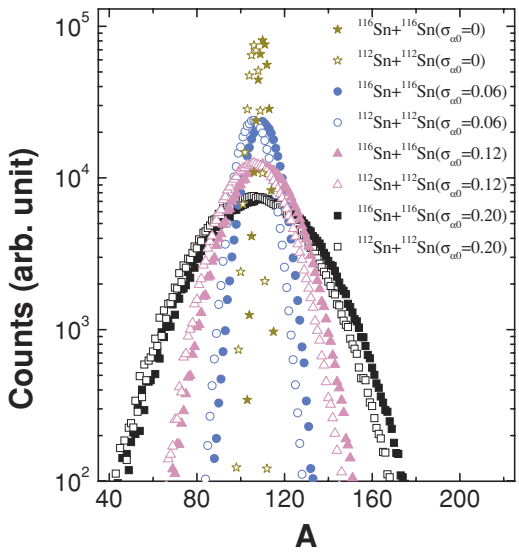

FIG. 2. (Color online) Fission-fragment mass distributions produced by the Langevin simulation for the reactions of ^{112}Sn+^{112}Sn (open symbols) and ^{116}Sn+^{116}Sn (filled symbols) at 8.4 MeV/nucleon with the different sampling width σ_{α_0} of Gaussian probability distribution.

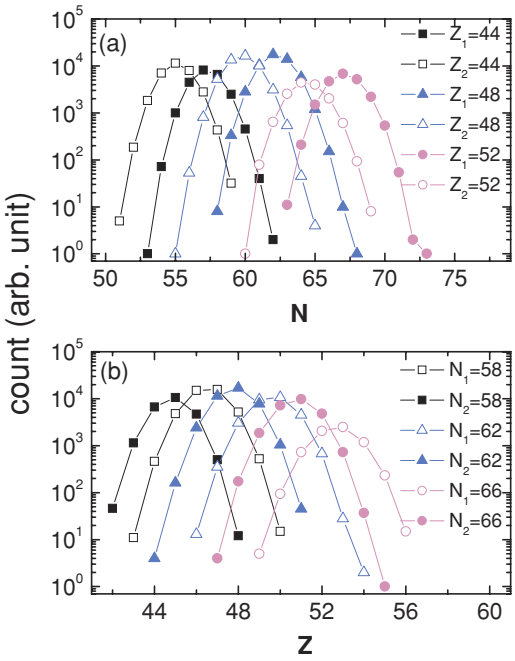

FIG. 3. (Color online) Isotopic (a) and isotonic (b) distributions of fission fragments in some given Z or N from the collisions of ^{116}Sn+^{116}Sn (filled symbols) and of ^{112}Sn+^{112}Sn (open symbols) at 8.4 MeV/nucleon. $\sigma_{\alpha_0} = 0.06$. Notice that the x-axis scale is different.

the mass asymmetrical parameter of fission fragments, but the differences of the centroid of the isotonic/isotopic distributions shows the dependence on it.

From a practical point of view, the isoscaling behavior occurs when two mass distributions for a given Z from two processes with different isospin are Gaussian distributions

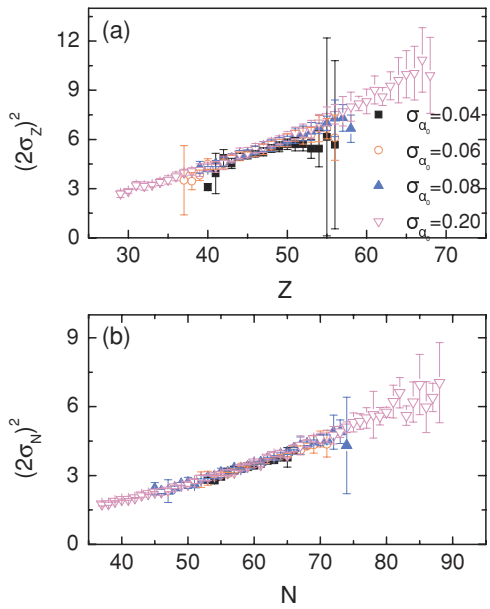

FIG. 4. (Color online) Square of full width of the isotopic (a) and isotonic (b) distribution as a function of Z and N, respectively, in different σ_{α_0}. The width is the average value of the two systems (they are almost the same for both systems).

with the same width but different mean mass. In this case, the isotopic distribution in a given Z, namely $Y(N)|_Z$, and isotonic distribution in a given N, namely $Y(Z)|_N$, can be described by a single Gaussian distribution, respectively, i.e.,

$$Y(N)|_Z \sim \exp\left[-\frac{(N-N_Z)^2}{2\sigma_Z^2}\right],$$
$$Y(Z)|_N \sim \exp\left[-\frac{(Z-N_N)^2}{2\sigma_N^2}\right], \tag{14}$$

where N_Z and N_N are the centroid of isotopic and isotonic distributions, and σ_Z^2 and σ_N^2 describe the variance of distributions for each element of charge Z and neutron number N, respectively. This leads to an exponential behavior of the ratio R_{21}. If the quadratic term in N_Z or N_N is neglected, it reads

$$\ln(R_{21}(N)|_Z) \sim \frac{[(N_Z)_2 - (N_Z)_1]N}{\sigma_Z^2},$$
$$\ln(R_{21}(Z)|_N) \sim \frac{[(N_N)_2 - (N_N)_1]Z}{\sigma_N^2}. \tag{15}$$

Note that Eq. (15) requires the values for σ_Z^2 or σ_N^2 to be approximately the same for both reactions, which is a necessary condition for isoscaling. Indeed, we observed this case in our simulations for both Sn+Sn collisions. In the Langevin equation, σ_Z^2 and σ_N^2 essentially depend on the physical conditions reached, such as the temperature, density, friction parameter, etc. Considering that $R_{21}(N)|_Z \sim \exp(\alpha N)$ or $R_{21}(Z)|_N \sim \exp(\beta Z)$ for a given Z or N, we can get

$$\alpha \sim \frac{(N_Z)_2 - (N_Z)_1}{\sigma_Z^2},$$
$$\beta \sim \frac{(N_N)_2 - (N_N)_1}{\sigma_N^2}. \tag{16}$$

Assuming other ingredients can be neglected, σ_Z^2 or σ_N^2 could be considered to be proportional to temperature T of the fission fragments according to the fluctuation-dissipation theorem [23]; in this circumstance,

$$\alpha \sim \frac{(N_Z)_2 - (N_Z)_1}{T},$$
$$\beta \sim \frac{(N_N)_2 - (N_N)_1}{T}, \tag{17}$$

where $[(N_Z)_2 - (N_Z)_1]$ and $[(N_N)_2 - (N_N)_1]$ can be understood as terms representing the average difference of the neutron or proton chemical potential between two reactions.

As we already showed, both σ_Z^2 and σ_N^2 rise with Z and N, respectively, and are almost independent of σ_{α_0} from Figs. 4(a) and 4(b) in our calculation. On the other hand, we recognize that the similar behavior of the Z dependence of σ_Z has been experimentally observed in the spallation-fission data of ^{208}Pb (1 GeV/nucleon) + d or p, etc., in Gesellschaft für Schwerionenforschung (GSI) [40,41]. According to the model which is based on the modern version of the abrasion-ablation model involving the fission nuclei by Benlliure *et al.* [42], the square of the width of the symmetric fission fragment from the

macroscopic potential can be expressed by

$$\sigma_Z^2 = \frac{1}{2}\frac{\sqrt{E^*_{\rm bf}}}{\sqrt{a}C_{\rm mac}} = \frac{T_{\rm fis}}{2C_{\rm mac}}, \qquad (18)$$

where $E^*_{\rm bf}$ is the excitation energy above the the fission barrier, a is the level energy parameter, $T_{\rm fis}$ is the temperature of fissioning nuclei, and $C_{\rm mac}$ is the curvature of macroscopic potential energy $V_{\rm mac}$ as a function of charge asymmetry. In this way, the width of symmetric fission fragment distribution increases with temperature. This is also the case in our present model calculation. In other words, the temperature of the fission fragments which mostly originates from the symmetric fission seems to increase with the charge number of the fragments. A recent systematic study of the experimental data also displays that the variance of the fragment mass distribution increases with the temperature of the compound nucleus and the fission fragments [43].

To verify this relationship between the temperature and the charge number of the fragments, we extract the temperature of the fissioning nuclei in the scission point when the system occurs on the dynamic channel. Figures 5(a) and 5(b) demonstrate the mean temperature of two systems as a function of Z and N for the fissioning nuclei, respectively. Obviously, the temperature almost increases linearly with the charge number $Z_{\rm fis}$ or neutron number $N_{\rm fis}$ of the fissioning nuclei. Since we assume the fission fragments have the same N/Z as the one of the fissioning nuclei, the temperature of the fission fragments shall increase with their charge number.

In Eq. (16), $[(N_Z)_2 - (N_Z)_1]$ and $[(N_N)_2 - (N_N)_1]$ can be understood as the average difference of the neutron or proton chemical potential between two reactions. Figures 6(a) and 6(b) show $[(N_Z)_2 - (N_Z)_1]$ and the absolute value of

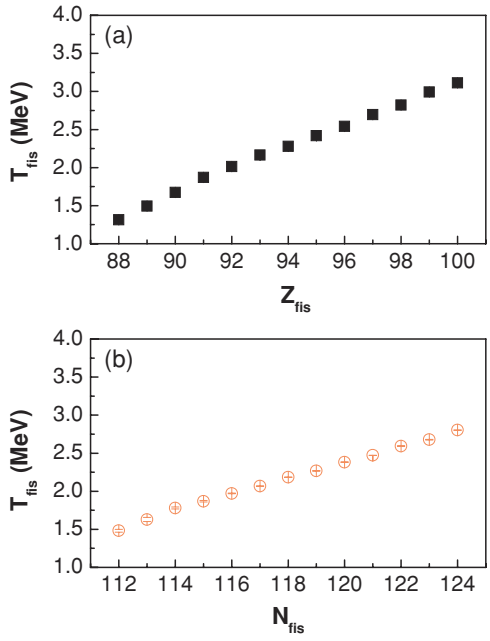

FIG. 5. (Color online) Extracted mean temperature of fissioning nuclei of two reaction systems as a function of their charge number (a) or neutron number (b).

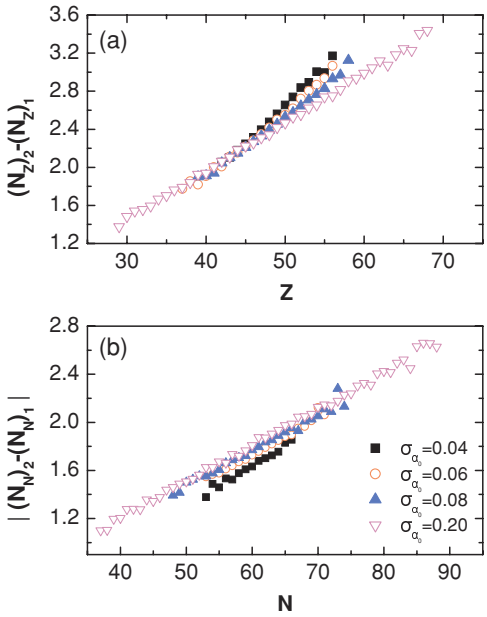

FIG. 6. (Color online)Values of $(N_Z)_2 - (N_Z)_1$ (a) and $|(N_N)_2 - (N_N)_1|$ (b) as a function of Z and N of the fission fragments, respectively, between ^{116}Sn+^{116}Sn and ^{112}Sn+^{112}Sn with different σ_{α_0}.

$[(N_N)_2 - (N_N)_1]$ as functions of Z or N, respectively, in different σ_{α_0}. Apparent increasing behavior with Z or N has been observed. In order to understand the increasing behavior of $[(N_Z)_2 - (N_Z)_1]$ or $|[(N_N)_2 - (N_N)_1]|$ as a function of the charge number and the neutron number of fission fragments, we investigate the fissioning nuclei. For example, Fig. 7(a) shows the neutron number vs the charge number of the fissioning nucleus for both reaction systems just before fission takes place. The lines represent the second-order polynomial fits to guide the eyes. From the above points, we can extract the $[(N_Z)_2 - (N_Z)_1]_{\rm fis}$ as a function of $Z_{\rm fis}$ as shown in Fig. 7(b). Since the fission fragments are assumed to have the same N/Z as one of the fissioning nuclei, the fission fragments will show a similar increasing behavior as the charge number rises. In comparison to the insensitivity of σ_Z or σ_N to σ_{α_0}, $[(N_Z)_2 - (N_Z)_1]$ and $[(N_N)_2 - (N_N)_1]$ show somewhat stronger dependences on σ_{α_0}, i.e., $[(N_Z)_2 - (N_Z)_1]$ has larger values in the proton-rich side while $|[(N_N)_2 - (N_N)_1]|$ shows smaller values in the neutron-deficit side as σ_{α_0} becomes smaller in Fig. 6. This essentially originates from the overlap of the different mass partitions of two fission fragments according to the sampling of the Gaussian probability distribution for the mass asymmetry when fission takes place. The symmetric fissions result in the strongest dependence of $[(N_Z)_2 - (N_Z)_1]$ and $|[(N_N)_2 - (N_N)_1]|$ on the charge number or neutron number.

B. Isoscaling behavior

Eq. (1) can be written as $\ln R_{21} = C_Z + \alpha N$, where $C_Z = \ln C + \beta Z$; if we plot R_{21} as a function of N on a natural logarithmic plot, the ratio follows a straight line. In Fig. 8, this

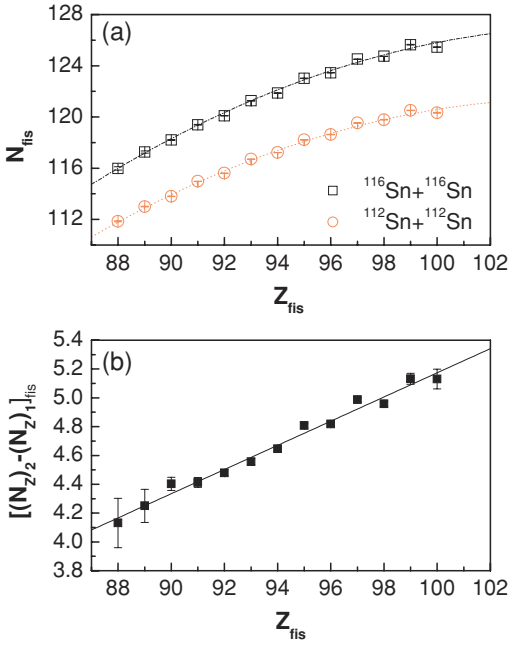

FIG. 7. (Color online) (a) Calculated neutron numbers as a function of the charge numbers for the fissioning nuclei of two reaction systems. (b) Difference of the neutron number of the fissioning nuclei between two reaction systems as a function of the charge number for the fissioning nuclei. Lines represent two-order polynomial fits in (a) and a linear fit in (b).

isoscaling behavior is observed in the Langevin simulation. Here each symbol with a line represents isotope an chain. From there, the isoscaling parameter α can be extracted directly. Similarly, the isoscaling parameter β can be extracted from the isotonic ratio as shown in Fig. 9 by $\ln R_{21} = C_N + \beta Z$, where $C_N = \ln C + \alpha N$.

From Figs. 8 and 9, the relationship between $\alpha(|\beta|)$ and the charge number $Z(N)$ of the fission fragments can be deduced.

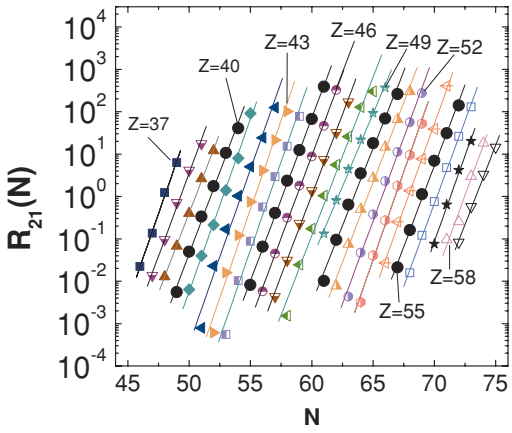

FIG. 8. (Color online) Isotopic yield ratio of fission fragments between ^{116}Sn+^{116}Sn and ^{112}Sn+^{112}Sn in the Langevin model with $\sigma_{\alpha_0} = 0.06$ and $E_{\text{beam}}/\text{A} = 8.4$ MeV. Different symbols from left to right represent the calculated results for the isotopes from $Z = 37$ to 59. The lines represent exponential fits to guide the eye.

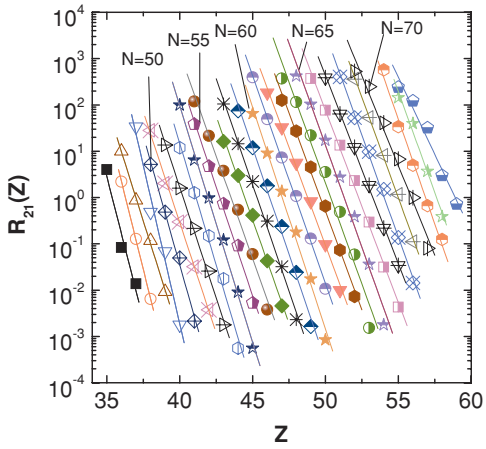

FIG. 9. (Color online) Same as Fig. 8, but for the isotonic yield ratio and $N = 46$–73.

In order to investigate the effect of the width of the Gaussian probability distribution on the isoscaling parameters, we use the different widths of the sampling Gaussian distribution for mass asymmetry parameter α_0, namely, $\sigma_{\alpha_0} = 0.04$, 0.06, 0.08, and 0.20, with the random number from -1 to 1 and the mean value of 0. Figure 10(a) shows the isoscaling parameter α as a function of Z with different σ_{α_0}. From this figure, we know that at low σ_{α_0}, i.e., when the symmetric fission is the overwhelming mechanism, α increases with Z. This means that the isospin effect becomes stronger as Z increases. A recent analysis of fission with a simple liquid-drop model [8] predicted a systematic increase of the isoscaling parameter α with the proton number of the fragment element. In our

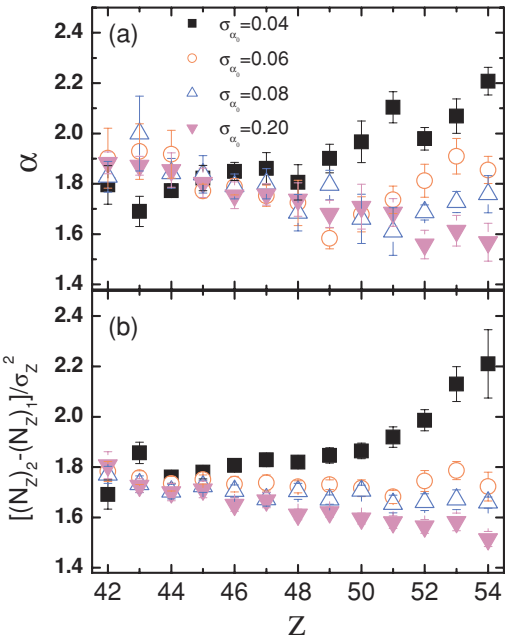

FIG. 10. (Color online) (a) Isoscaling parameter α as a function of Z in the different Gaussian widths σ_{α_0} of the mass asymmetry parameter α_0 for fission fragments; (b) same as (a), but for $\frac{[(N_Z)_2-(N_Z)_1]}{\sigma_Z^2}$.

simulation, this kind of increase of α with Z apparently stems from the dominant symmetric fission mechanism. However, in the other extreme in Fig. 10(a), i.e., at a large σ_{α_0}, α shows a contrary trend with Z; i.e., it drops with increasing Z. In this case, it seems that there exists a stronger isospin effect for the fragments with lower Z. In a midrange case, the rising and falling branches compete with each other, the mediate isoscaling behavior appears, and a minimum α parameter occurs around the symmetric fission point. We note that the fission data of ^{238,233}U targets induced by 14 MeV neutrons reveal the same backbending behavior of the isoscaling parameter α around the symmetric fission point [9] as just described. They interpreted the behavior as originating from the temperature difference of fission fragments since the isoscaling parameter is typically, within the grand-canonical approximation, considered inversely proportional to the temperature ($\alpha = \Delta\mu_n/T$) as stated above. In our case, this kind of backbending of isoscaling parameter α apparently stems from the moderate width of the probability distribution of the mass asymmetrical parameter of the fissioning nucleus as shown in Fig.10. In other words, it may stem from a moderate mixture of the different weights between the symmetric and asymmetric fission components. Essentially, the backbending originates from the competition between the chemical potential and the temperature since both parameters increase with the charge number of fission fragments.

Besides the above direct method for extracting an isoscaling parameter, we can also check the behavior of α in terms of Eq. (17). Figure 10(b) shows $\frac{[(N_Z)_2-(N_Z)_1]}{\sigma_Z^2}$ as a function of Z. With increasing σ_{α_0}, the Z dependence of $\frac{[(N_Z)_2-(N_Z)_1]}{\sigma_Z^2}$ shows from the upswing trend to the downswing trend. A turning point at $Z = 51$ is also observed in medium σ_{α_0}, as Fig. 10(a) shows. From the similarity of the behavior shown in Figs. 10(a) and 10(b) as well as the approximate equality of the values of α and $\frac{[(N_Z)_2-(N_Z)_1]}{\sigma_Z^2}$, we can say that Eq. (17) works well in the present calculation. In our case, the turning point of α stems from the competition between the chemical potential term $[(N_Z)_2 - (N_Z)_1]$ and the temperature term σ_Z^2. In general, the chemical potential term is more sensitive to the Gaussian width of the mass asymmetry parameter α_0 for fission fragments (see Fig. 6). Overall, we find that the isoscaling parameter α is sensitive to the width of the probability distribution of mass asymmetrical parameter of the fission fragments. In other words, we may say that the isoscaling parameter is sensitive to the asymmetrical extent of both fission fragments.

Similarly, from Fig. 9, the relationship between $|\beta|$ and the neutron number N of the fission fragments can be deduced for different widths σ_{α_0}. This is shown in Fig. 11(a). Different from the relationship of α and Z, the $|\beta|$ always drops as the neutron number increases, regardless of the change of σ_{α_0}. The quantitative and qualitative similarity of $\frac{[(N_N)_2-(N_N)_1]}{\sigma_N^2}$ vs N [Fig. 11(b)] has also been observed; i.e., it always decreases with increasing N and is insensitive to σ_{α_0}.

However, the obtained isoscaling parameters are actually very large in comparison to the usual isoscaling parameter extracted from the data [9]. The reasons could be the model itself, since the model is still too simple, or our assumption of a

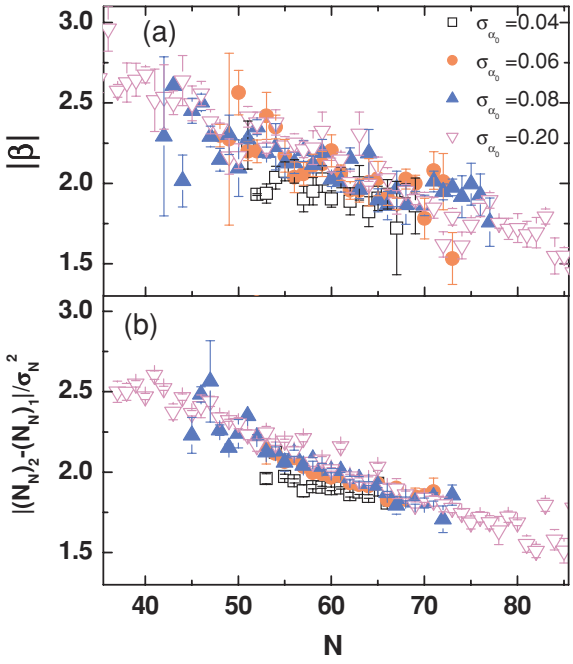

FIG. 11. (Color online) (a) Isoscaling parameter $|\beta|$ as a function of Z in the different Gaussian widths σ_{α_0} of the mass asymmetry parameter α_0 for fission fragments; (b) same as (a), but for $|\frac{(N_N)_2-(N_N)_1}{\sigma_N^2}|$.

Gaussian probability distribution of the fission fragments. Also the post-fission evaporation component will, of course, play some role in modification of the isoscaling parameters. The present model calculation, however, does not include this influence of post-fission evaporation of fission fragments. Those factor may result in larger apparent isoscaling parameters in comparison to the data. Of course, the main aim of this work is to show the isoscaling behavior of fission fragments and its trend with the charge or neutron number of the fragments by the Langevin dynamics.

C. The beam energy dependence of the isoscaling parameters

The simulations are systematically performed for different beam energies. The values of α and $|\beta|$ are extracted as a function of beam energy for the fragments $Z = 44$–54 and $N = 58$–68, respectively, as shown in Figs. 12(a) and 12(b). It shows that both α and β decrease as the beam energy increases, which means that the isospin effect fades away with increasing E_{beam}/A. This behavior is similar to the fragmentation case in which the isoscaling parameter drops with increasing temperature in the statistical models as well as experiments [6,16,38,44].

D. The friction parameter dependence of the isoscaling parameters

In addition, the influence of the reduced friction parameter on the isoscaling parameters is investigated; we use a constant value of $\beta_0 = 2, 4, 6, 8$, and 10 instead of the one-body

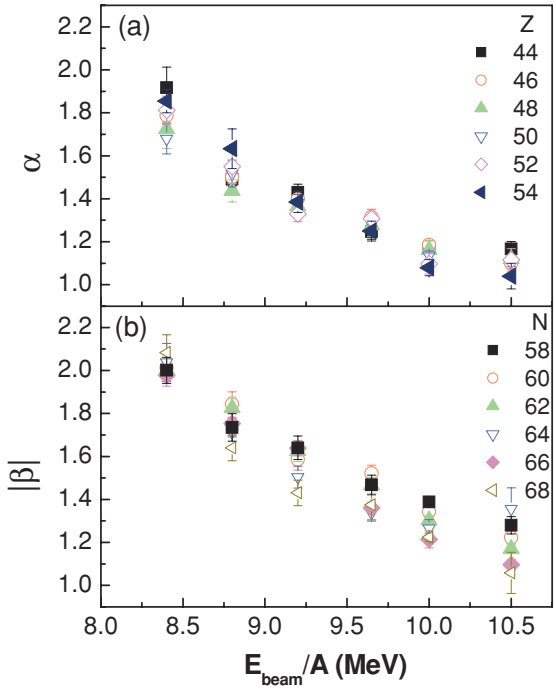

FIG. 12. (Color online) Isoscaling parameter α (a) and $|\beta|$ (b) as functions of beam energy for the fragments $Z = 44$–54 and $N = 58$–68, respectively. The width σ_{α_0} of the Gaussian probability is 0.06.

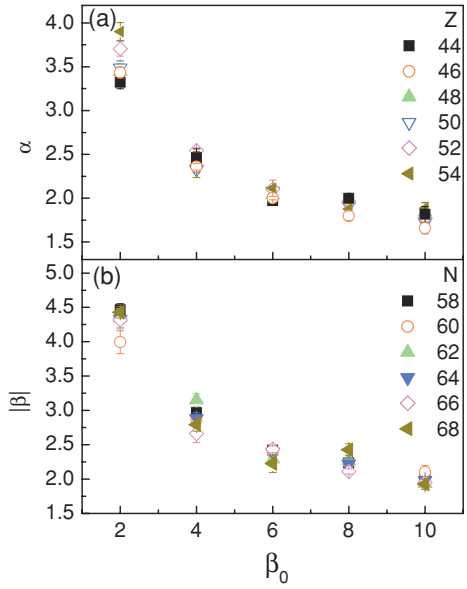

FIG. 13. (Color online) Same as Fig. 12, but plotted against the reduced friction parameter β_0.

dissipation β_{OBD} used earlier. In Figs. 13(a) and 13(b), we plot α and $|\beta|$ as a function of β_0 for different elements from $Z = 44$ to 54 or different isotones from $N = 58$ to 68, respectively. Both α and $|\beta|$ decrease as the reduced friction parameter increases. It shows that α and β are sensitive to the reduced friction parameter. Larger reduced friction makes the Brownian particles spend more energy which is transferred to the internal energy from ground state to the scission point, than does the smaller reduced friction. Consequently, the system will keep less memory at the initial entrance channel. As for the isoscaling behavior, the isoscaling parameter also shows a decrease with the larger reduced friction parameter. Therefore, the study of the isoscaling behavior of the fission fragment might be a good tool for exploring the friction effect in the fission dynamics process.

IV. SUMMARY

In summary, we applied the Langevin model to investigate the isoscaling behavior in the dynamical process of compound nuclear fission. In order to treat the fission fragments, we assume that the mass asymmetry parameter of the two fission fragments from the fissioning nucleus is taken from a random number with a Gaussian distribution whose width is σ_{α_0}. The simulation illustrates that the isotopic and isotonic yield ratios of fission fragments in the dynamical fission channels of the ^{116}Sn+^{116}Sn and ^{112}Sn+^{112}Sn reaction systems show the isoscaling behavior. The terms which are related to the difference of neutron or proton chemical potential are also extracted. It is interesting that the isoscaling parameter α is strongly sensitive to the Gaussian width σ_{α_0} of the mass asymmetry parameter but β is not. When σ_{α_0} is small, i.e., the fission is almost symmetric, α increases with the atomic number of fission fragments, which is similar to the theoretical prediction of a simple liquid-drop model [8]. In contrast, when σ_{α_0} is large, for instance, $\sigma_{\alpha_0} = 0.20$, α drops with increasing Z of fission fragments. However, in the intermediate values of σ_{α_0}, α shows a backbending with Z of fission fragments, which is similar to the observation of the ^{238,233}U fission data induced by 14 MeV neutrons [9]. In this context, we could say that the α parameter is sensitive to the asymmetric extent of the fission fragments from the fissioning nuclei. However, β parameter is insensitive to the width σ_{α_0} even though it always shows the dropping trend with N.

In addition, the dependences of beam energy and the reduced friction parameter for the isoscaling parameters are systematically investigated. It is found that both α and β drop with increasing beam energy of the projectile as well as the reduced friction parameter, reflecting the temperature-like dependence of isoscaling parameters in the fission dynamics. The disappearance of isospin effect of fission dynamics is expected in a certain higher beam energy or larger reduced friction parameter. In general, the isoscaling analysis of the fission data appears to be a sensitive tool for investigating the fission dynamics.

ACKNOWLEDGMENTS

This work was supported in part by the Shanghai Development Foundation for Science and Technology under Grant Nos. 05XD14021 and 03QA14066, the National Natural Science Foundation of China under Grant Nos. 10328259, 10135030, and 10405033, and the Major State Basic Research Development Program under Contract No. G200077404.

[1] *Isospin Physics in Heavy-Ion Collisions at Intermediate Energies*, edited by B.-A. Li and W. U. Schroeder (NOVA Science, New York, 2001).

[2] R. Wada, K. D. Hildenbrand, U. Lynen, W. F. J. Müller, H. J. Rabe, H. Sann, H. Stelzer, W. Trautmann, R. Trockel, N. Brummund, R. Glasow, K. H. Kampert, R. Santo, E. Eckert, J. Pochodzalla, I. Bock, and D. Pelte, Phys. Rev. Lett. **58**, 1829 (1987).

[3] S. J. Yennello, B. Young, J. Yee, J. A. Winger, J. S. Winfield, G. D. Westfall, A. Vander Molen, B. M. Sherrill, J. Shea, E. Norbeck, D. J. Morrisseya, T. Lia, E. Gualtieria, D. Craiga, W. Benensona, and D. Bazina, Phys. Lett. **B321**, 15 (1994).

[4] M. B. Tsang, W. A. Friedman, C. K. Gelbke, W. G. Lynch, G. Verde, and H. Xu, Phys. Rev. Lett. **86**, 5023 (2001).

[5] M. B. Tsang, W. A. Friedman, C. K. Gelbke, W. G. Lynch, G. Verde, and H. S. Xu, Phys. Rev. C **64**, 041603(R) (2001).

[6] M. B. Tsang, C. K. Gelbke, X. D. Liu, W. G. Lynch, W. P. Tan, G. Verde, H. S. Xu, W. A. Friedman, R. Donangelo, S. R. Souza, C. B. Das, S. Das Gupta, and D. Zhabinsky, Phys. Rev. C **64**, 054615 (2001).

[7] Y. G. Ma, H. Y. Zhang, and W. Q. Shen, Prog. Phys. (Chin.) **22**, 99 (2002); Y. G. Ma and W. Q. Shen, Nucl. Sci. Technol. **15**, 4 (2004).

[8] W. A. Friedman, Phys. Rev. C **69**, 031601(R) (2004).

[9] M. Veselsky, G. A. Souliotis, and M. Jandel, Phys. Rev. C **69**, 044607 (2004).

[10] G. A. Souliotis, D. V. Shetty, M. Veselsky, G. Chubarian, L. Trache, A. Keksis, E. Martin, and S. J. Yennello, Phys. Rev. C **68**, 024605 (2003).

[11] M. Veselsky, G. A. Souliotis, and S. J. Yennello, Phys. Rev. C **69**, 031602(R) (2004).

[12] T. X. Liu, X. D. Liu, M. J. van Goethem, W. G. Lynch, R. Shomin, W. P. Tan, M. B. Tsang, G. Verde, A. Wagner, H. F. Xi, H. S. Xu, M. Colonna, M. Di Toro, M. Zielinska-Pfabe, H. H. Wolter, L. Beaulieu, B. Davin, Y. Larochelle, T. Lefort, R. T. de Souza, R. Yanez, V. E. Viola, R. J. Charity, and L. G. Sobotka, Phys. Rev. C **69**, 014603 (2004).

[13] E. Geraci, M. Bruno, M. D'Agostino, E. De Filippo, A. Pagano, G. Vannini, M. Alderighi, A. Anzalone, L. Auditore, V. Baran, R. Barna, M. Bartolucci, I. Berceanu, J. Blicharska, A. Bonasera, B. Borderie, R. Bougault, J. Brzychczyk, G. Cardella, S. Cavallaro, A. Chbihi, J. Cibor, M. Colonna, D. De Pasquale, M. Di Toro, F. Giustolisi, A. Grzeszczuk, P. Guazzoni, D. Guinet, M. Iacono-Manno, A. Italiano, S. Kowalski, E. La Guidara, G. Lanzalone, G. Lanzano, N. Le Neindre, S. Li, S. Lo Nigro, C. Maiolino, Z. Majka, G. Manfredi, T. Paduszynski, M. Papa, M. Petrovici, E. Piasecki, S. Pirrone, G. Politi, A. Pop, F. Porto, M. F. Rivet, E. Rosato, S. Russo, P. Russotto, G. Sechi, V. Simion, M. L. Sperduto, J. C. Steckmeyer, A. Trifiro, M. Trimarchi, M. Vigilante, J. P. Wieleczko, J. Wilczynski, H. Wu, Z. Xiao, L. Zetta, and W. Zipper, Nucl. Phys. **A732**, 173 (2004).

[14] W. D. Tian, Y. G. Ma, X. Z. Cai, J. G. Chen, J. H. Chen, D. Q. Fang, W. Guo, C. W. Ma, G. L. Ma, W. Q. Shen, K. Wang, Y. B. Wei, T. Z. Yan, C. Zhong, and J. X. Zuo, nucl-th/0411097, Chin. Phys. Lett. **22**, 306 (2005).

[15] A. Ono, P. Danielewicz, W. A. Friedman, W. G. Lynch, and M. B. Tsang, Phys. Rev. C **68**, 051601(R) (2003).

[16] Y. G. Ma, K. Wang, Y. B. Wei, G. L. Ma, X. Z. Cai, J. G. Chen, D. Q. Fang, W. Guo, W. Q. Shen, W. D. Tian, and C. Zhong, Phys. Rev. C **69**, 064610 (2004).

[17] A. S. Botvina, O. V. Lozhkin, and W. Trautmann, Phys. Rev. C **65**, 044610 (2002).

[18] S. R. Souza, R. Donangelo, W. G. Lynch, W. P. Tan, and M. B. Tsang, Phys. Rev. C **69**, 031607(R) (2004).

[19] K. Wang, Y. G. Ma, Y. B. Wei, X. Z. Cai, J. G. Chen, D. Q. Fang, W. Guo, G. L. Ma, W. Q. Shen, W. D. Tian, C. Zhong, and X. F. Zhou, Chin. Phys. Lett. **22**, 53 (2005).

[20] P. Fröbrich and I. I. Gontchar, Phys. Rep. **292**, 131 (1998).

[21] I. I. Contchar, L. A. Litnevsky, and P. Fröbrich, Comput. Phys. Commun. **107**, 223 (1997).

[22] J. Randrup, Nucl. Phys. **A327**, 490 (1979).

[23] H. Feldmeier, Rep. Prog. Phys. **50**, 915 (1987).

[24] H. Hofmann, Phys. Rep. **284**, 137 (1997).

[25] P. Möller, W. D. Myers, W. J. Swiatecki, and J. Treiner, At. Data Nucl. Data Tables **39**, 225 (1998).

[26] A. V. Ignatyuk *et al*., Fiz. Elem. Chastits At. Yadra **16**, 709 (1985).

[27] W. D. Myers and W. J. Swiatecki, Nucl. Phys. **81**, 1 (1996); Ark. Fys. **36**, 343 (1967).

[28] R. W. Hasse and W. D. Myers, *Geometrical Relationships of Macroscopic Nuclear Physics* (Springer, Berlin, 1988).

[29] R. L. Stranovich, *Topics in the Theory of Random Noise*, Vols. I and II (Gorden & Beach, New York, 1967).

[30] I. I. Gontchar, Fiz. Elem. Chastits At. Yadra **26**, 932 (1995).

[31] H. Risken, *The Fokker-Planck Equation*, 2nd ed. (Springer, Berlin, 1989).

[32] Yu. L. Klimontovich, Phys. Uspekhi **37**, 737 (1994).

[33] J. Blocki, Y. Boneh, J. R. Nix, J. Randrup, M. Robel, A. J. Sierk, and W. J. Swiatecki, Ann. Phys. (NY) **113**, 330 (1978).

[34] I. I. Gontchar and L. A. Litnevsky, Z. Phys. A **26**, 347 (1997).

[35] M. Blann, Phys. Rev. C **21**, 1770 (1980).

[36] J. E. Lynn, *Theory of Neutron Resonance Reactions* (Clarendon, Oxford, 1968).

[37] Y. G. Ma, Q. M. Su, W. Q. Shen, J. S. Wang, X. Z. Cai, and D. Q. Fang, Chin. Phys. Lett. **16**, 256 (1999).

[38] Y. G. Ma, Q. M. Su, W. Q. Shen, D. D. Han, J. S. Wang, X. Z. Cai, D. Q. Fang, and H. Y. Zhang, Phys. Rev. C **60**, 024607 (1999).

[39] B. Gatty, D. Guerreau, M. Lefort, J. Pouthas, X. Tarrago, J. Galin, B. Cauvin, J. Girard, and H. Nifenecker, Z. Phys. A **273**, 65 (1975).

[40] T. Enqvist, P. Armbruster, J. Benlliure, M. Bernas, A. Boudard, S. Czajkowski, R. Legrain, S. Leray, B. Mustapha, M. Pravikoff, F. Rejmund, K.-H. Schmidt, C. Stéphan, J. Taieb, L. Tassan-Got, F. Vivés, C. Volant, and W. Wlazlo, Nucl. Phys. **A703**, 435 (2002).

[41] M. Bernas, P. Armbruster, J. Benlliure, A. Boudard, E. Casarejos, S. Czajkowski, T. Enqvist, R. Legrain, S. Leray, B. Mustapha, P. Napolitani, J. Pereira, F. Rejmund, M.-V. Ricciardi, K.-H. Schmidt, C. Stéphan, J. Taieb, L. Tassan-Got, and C. Volant, Nucl. Phys. **A725**, 213 (2003).

[42] J. Benlliure, A. Grewe, M. de Jong, K.-H. Schmidt, and S. Zhdanov, Nucl. Phys. **A628**, 458 (1998).

[43] Y. S. Sawant, A. Saxena, R. K. Choudhury, P. K. Sahu, R. G. Thomas, L. M. Pant, B. K. Nayak, and D. C. Biswas, Phys. Rev. C **70**, 051602(R) (2004).

[44] Y. G. Ma, Acta Phys. Sin. **49**, 654 (1999).